

In Memoriam

of E.P. Abranin and L.L. Baselyan

DOI: <https://doi.org/10.15407/rpra28.03.183>

UDC 523.985.7-77+523.947+520.27

A.A. Stanislavsky¹, A.A. Koval², I.N. Bubnov¹, and A.I. Brazhenko³

¹ Institute of Radio Astronomy NAS of Ukraine

4, Mystetstv St., Kharkiv, 61002, Ukraine

E-mail: a.a.stanislavsky@rian.kharkov.ua

² Astronomical Institute of the Czech Academy of Sciences

Fričova 298, 251 65 Ondřejov, Czech Republic

³ Poltava Gravimetric Observatory, Subbotin Institute of Geophysics NAS of Ukraine

27/29, Myasoyedov St., Poltava, 36029, Ukraine

PROGRESS IN THE STUDY OF DECAMETER-WAVELENGTH SOLAR RADIO EMISSION WITH UKRAINIAN RADIO TELESCOPES. Part 2*

Subject and Purpose. *This part of the paper continues presentation of results of the solar radio emission studies performed with Ukrainian radio telescopes over the past 20 years. The importance is stressed of developing adequate instruments and methods for identifying the nature of decameter-wavelength radio emissions from the Sun.*

Methods and Methodology. *The low frequency Ukrainian radio telescopes UTR-2, GURT and URAN-2 have been used in the project along with other ground- and space based instruments in order to achieve a comprehensive understanding of physical conditions in the solar corona.*

Results. *Special methods and tools have been developed for studying radio frequency burst emissions against the background of strong interference. Unique data have been obtained concerning sources of sporadic radio emissions from the Sun, as well as the contribution from wave propagation effects and the impact of the ionosphere on the results of observations. The most significant observational and theoretical results are presented, obtained in the study of solar low frequency emissions over the past 20 years. Solar radio emissions are shown to be efficient sounding signals not for the solar corona alone but for the Earth's ionosphere as well, which allows identifying its impact on the results of radio astronomy observations.*

Conclusions. *The Ukrainian radio telescopes of the meter and decameter wavebands currently are unrivalled tools for investigating the Universe in the low-frequency range of radio waves. Owing to their advanced characteristics, they make a significant contribution to the progress of world's solar radio astronomy.*

Keywords: *the Sun, decameter-wavelength radio emission, radio bursts, solar corona, UTR-2, URAN-2, GURT.*

* Invited paper.

Citation: Stanislavsky, A.A., Koval, A.A., Bubnov, I.N., and Brazhenko, A.I., 2023. Progress in the study of decameter-wavelength solar radio emission with Ukrainian radio telescopes. Part 2. *Radio Phys. Radio Astron.*, 28(3), pp. 183–200. <https://doi.org/10.15407/rpra28.03.183>

Ц и т у в а н н я: Станіславський О.О., Коваль А.О., Бубнов І.М., Браженко А.І. Досягнення у вивченні декаметрового радіо-випромінювання Сонця за допомогою українських радіотелескопів. Частина 2. *Радіофізика і радіоастрономія*. 2023. Т. 28. № 3. С. 183–200. <https://doi.org/10.15407/rpra28.03.183>

© Publisher PH "Akademperiodyka" of the NAS of Ukraine, 2023. This is an open access article under the CC BY-NC-ND license (<https://creativecommons.org/licenses/by-nc-nd/4.0/>)

© Видавець ВД «Академперіодика» НАН України, 2023. Статтю опубліковано відповідно до умов відкритого доступу за ліцензією CC BY-NC-ND (<https://creativecommons.org/licenses/by-nc-nd/4.0/>)

Introduction

Part 2 of this paper continues the overview of the results obtained in the study of decameter-wavelengths solar radio emission that was performed with Ukrainian radio telescopes. We believe our results to be significant as they confirm many of the previous findings in a completely independent way. Moreover, our instruments are just the few in the world, capable of operating at extremely low frequencies. The subjects of this paper include features of drift pairs; observations of the solar radio emissions focused on ionospheric disturbances; simultaneous observations performed with space- and ground-based instruments, etc., all of which open new possibilities for interpreting solar events. In addition we have developed new antennas, useful for radio observations below 8 MHz. This allowed us to be the first observers to have detected an association of a solar U-type burst with type III bursts. Moreover, this paper outlines new prospective studies of the decameter-wavelength solar radio emissions with the help of Ukrainian radio telescopes.

1. Drift Pairs

1.1. Preliminary studies with a 60-channel spectrometer

Solar "drift pair" (DP) bursts were discovered by Roberts in 1958. The DPs are detectable with ground-based instruments at decameter and meter wavelengths (from the ionospheric cut-off frequency and up to 80 MHz). Their characteristic features are shown in special morphological forms presented in dynamic spectra of the records. Specifically, they consist of two narrow components separated in time, often the later one being a replica of the former (Fig. 1). The bursts are characterized by limited frequency bandwidths, while showing a noticeable frequency drift. Furthermore, the drift rate may be either positive or negative. Typically, the DPs are observed during type III solar burst storms, however not every storm leads to the appearance of DPs. Note also that DPs do not occur as often as type III bursts. Unfortunately, the several theories existing today can but only partially explain the properties of these bursts.

The DPs observed with the UTR-2 back in the 1970s involved two narrow frequency bands (of

widths about 1 to 2 MHz). An attempt of performing a more comprehensive analysis of such bursts over a continuous frequency band of 10 to 30 MHz was undertaken in July, 2002, with the use of a 60-channel radiometer. The disadvantages of that equipment have already been considered here (see Section 4 of Part 1). They had a rather negative impact on the results. In particular, the frequency drift rates of 776 DPs were supposed to be describable by the formula $df/dt = -A(f/f_0)^B + C$, with f_0 being equal to 25 MHz, and A , B and C representing fitting parameters. Upon application of least-squares approximation procedures these parameters took the following values: $A = -0.5$, $B = 2.7$ and $C = -0.4$ for the forward DPs (FDPs), and $A = 2.3$, $B = 6.2$ and $C = 1$ for the reverse (RDPs). Further observations of the solar DPs, performed with a UTR-2 telescope equipped with numerical receivers, showed those results to be erroneous [1–4]. So, we aim now at considering those studies in more detail.

1.2. Observations of 2015

In the UTR-2 observations of July 10 to 12, 2015 we have detected 301 DP bursts, 92 of which were RDPs and 209 were FDPs [1]. All of them were recorded with the digital receiver/spectrometer possessing time resolution of 50 ms and a 4 kHz frequency resolution over 9–33 MHz (Fig. 1). The emergence of DPs and of the type III burst storms were associated in those days with the presence of a most active region, namely NOAA AR 12381 (N14W25 on 10 July of 2015). The day before it was located near the central solar meridian. The sunspot group of magnetic class β involved spots of both positive and negative magnetic polarity, with a simple division between them. The solar activity was accompanied by rare solar class C X-ray flares. The DP bursts differed in parameters, such as frequency bandwidth, start and end frequencies, time duration and frequency drift rates. One of DP parameters of interest is the width of the total frequency band occupied by each of such bursts [2]. We have analysed the characteristics of the FDPs and RDPs measured on July 10–12, 2015. The average value of the frequency bandwidth was 2.82 ± 1.32 MHz for RDPs, whereas for FDPs it was 3.6 ± 2.4 MHz. It is important to note that our observations of those days clearly showed the high-frequency edges of long DPs to be located near the

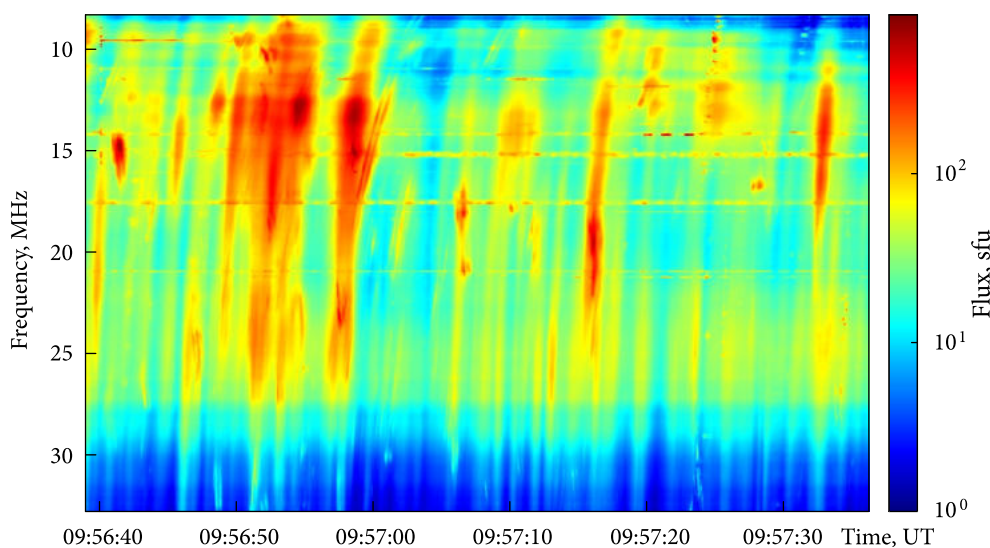


Fig. 1. Dynamic spectrum of the solar drifting pairs observed July 11, 2015 with the UTR-2 radio telescope

upper limit of the UTR-2 frequency band. Unfortunately, those observations did not permit recording the radio emissions over the entire frequency band that the DPs originated in. This imposes restrictions on our measured results. Within the observation frequency range pertinent to our instrument, the number of FDPs decreased at higher frequencies, whereas that of RDPs reduced toward lower frequencies. As it can be seen from the histogram analysis, the number of RDPs increases toward higher frequencies, while the FDPs show a similar trend toward lower frequencies. These features can be characterized in terms of the skewness parameter, as a measure of asymmetry in probabilistic distributions. In the case of FDPs the parameter is equal to 0.237, while for RDPs it is -0.966 . Unfortunately, the frequency range of the DP observations was not sufficient for performing a complete study of the FDP and RDP distributions. It is not surprising that in our observations of year 2002 the FDP – RDP relations looked like 109 vs 89 on July 13, and 186 vs 123 on July 14. In this context any observation performed at lower frequencies than had been done before should be of essential interest for the analysis of FDPs. However, capabilities of the ground-based instruments are limited by the ionosphere (recall the cutoff-associated effects). As for investigations on board of spacecraft, they cannot provide acceptable levels of time- and frequency resolution for studying DPs, and in addition their sensitivity is not high enough, the antennas being too simple.

While studying the histograms of DP bandwidths and the quantile-quantile plots, we have found that the probability density function (PDF) belongs to the Pearson III type. The presence of FDPs seems more likely at lower observation frequencies, in contrast to the RDPs. Besides, at some frequencies the emergence of RDPs or FDPs appears almost equally probable. It is the reverse DPs that prevail above these frequencies, whereas below the forward DPs dominate. This is also confirmed by intersection effects in the corresponding histograms. Consequently, the intersection peak (at 20–25 MHz on July 10–12, 2015) corresponds to equal numbers of the FDPs and RDPs observed. In the case of RDPs the bursts were not detected below 12.1 MHz. A similar result was observed in 2002. Moreover, one can assume that FDPs were unlikely to occur below 1.33 MHz, since $\Pr(f < 1.33) \approx 4.7 \times 10^{-9}$. On the other hand, the DP bursts probably did not occur above 50 MHz during that observation session because of $\Pr(f > 50) \approx 2.4 \times 10^{-4}$. This opens up a possibility of detecting FDPs below the ionospheric cutoff. It also seems clear that the upper and the lower frequencies within which DP bursts are observed can vary from one type III burst storm to another.

The next analysis of DPs is devoted to their frequency drift properties. The data processing procedure was as follows. For each component of DPs we sought to identify the time moment t_i in each frequency channel f_i (within the frequency band, where the given DP was detected) that corresponded to

the "centre" of the intensity hump for the DP burst under consideration. Consequently, on the dynamic spectrum corresponding to that emission type each of such components traces out a line of its own, which characterizes the frequency drift of the chosen DP. The frequency channels of the digital records that were damaged by narrow-band radio interference were ignored. Because of signal fluctuations, the peak points (t_i, f_i) of the DPs quite often could not be ascribed to a smooth curve. Next, we have chosen a power-law function to fit the evolution of these burst peaks on the frequency-time plane. This approach is similar to the concept used for the study of type III bursts. In this case the frequency drift rate satisfies the relation $df/dt = Kf^\nu$, where K and ν are constant magnitudes. Note that this dependence includes two parameters rather than three, as was suggested for the 2002 observations performed with the 60-channel analog receiver/spectrometer. Such a three-parameter model is not correct, which leads to "overfitting" in the data analysis. The frequency drift rates of each DP are described separately for each of its components, in terms of their specific values of K and ν . It should be pointed out that DPs can occur at different times. The long DPs are most convenient for this analysis [3]. In particular, the number of such pairs recorded in our observational session equaled 21 (20 FDPs and just one RDP), and their the frequency bandwidths varied between ~ 8 and 15 MHz. Based on the processing procedure, we have analysed frequency drift rates of both forward and reverse DPs. Note the characteristics of DPs to change with frequency in a similar way to such of type III bursts whose drift rate decreases with frequency. Each DP is characterized by frequency drift rates of its components. These are slightly different in each pair, although the later component repeats the tendencies of the previous one, such that they are still a pair. As follows from the histograms, the K and ν parameters have skewed distributions. They are characterized by the mean value, mode and median which are different for the FDPs and RDPs.

One important feature of DPs is the delay time between the DPs components as shown for the same frequency, as well as their frequency separation shown at some fixed instant. According to the observational session of 2002 the values of delay time decreased slowly with frequency, varying from 1.4 s to 2.6 s. However, the results have provided an aver-

aged description for many DPs at 12 equidistant frequencies. Using the frequency drift properties of DPs considered above, we can study the frequency and time separations between pair components in each individual burst, providing higher time and frequency resolutions (50 ms and 4 kHz, respectively). For this purpose we used long DPs. Generally, they follow the tendency of a delay time decreasing with frequency. The frequency separation shows an opposite behaviour, i.e. the value increases with frequency. The tracks may often demonstrate a monotonic character, however sometimes their behaviour is similar to that of a function with a single local extremum.

1.3. Observations of 2017

The statistical analysis of DPs was continued with the use of the July 12, 2017 observations [4]. The data were obtained through measurements with the UTR-2, the URAN-2 array, a subarray of GURT, and a single active cross-dipole, and provided spectral properties of radio bursts in the frequency range of 8–80 MHz [5]. Note that the latter antenna was verified as an antenna prototype for future low-frequency radio telescopes on the Moon [6]. According to the space-based observations with STEREO, GOES and SOHO, on July 10–16, 2017, solar activity varied with time from a low level on July 11 and rather moderate on July 12, to high on July 14. Then the activity looked moderate again on July 15–16, and dropped down to low later. The majority of solar events were connected to the active region NOAA AR 12665. The dark core of the sunspot was larger than the Earth. After July 12 the active region 12665 decayed slowly and quietly. Note that during the observations of DPs on July 12, 2017 that active region was a bipolar sunspot group. A similar sunspot group was associated with the DPs observed in 2015 [2]. The data of 2017 included 760 DP bursts from which 550 were forward, and 210 were reverse. According to our consideration, the average value of frequency bandwidth was 3.31 ± 1.58 MHz for RDPs, whereas for FDPs it was 3.94 ± 2.38 MHz. There is a high correlation between the starting and ending DP frequencies (0.92 for FDPs and 0.95 for RDPs). This indicates that the frequencies at the start and end of the event are related. The histograms of low- and high-frequency edges in the FDPs and RDPs indicated right-skewed data that could be described by a right-skewed dis-

tribution with a long rightward tail in the positive direction. The skewness is real and was not caused by instrumental effects. Note that such behaviour is typical if the random variable cannot assume negative values.

An important advantage of the GURT observations is that the records from that instrument cover the frequency range where the RDPs arise nearly completely, plus partially covering the frequencies typical of the FDPs. Through a simple straightforward calculation of the number of DPs observed with the GURT on July 12 within the range of 30 to 70 MHz (unfortunately, the lower and the higher frequencies were clogged by interference), we have been able to detect 2602 DPs. Among these events 2178 were RDPs, and 424 were FDPs. It should be pointed out that the UTR-2 observations were carried out ± 3 hr before and after noon, whereas the GURT antenna allowed us observing the solar radiation for the longer period from sunrise to sunset. In particular, it is this fact that can explain the difference in the number of DPs observed with the latter instrument. From the location of the FDPs and RDPs on the frequency scale, the occurrence of FDPs seems more probable at lower frequencies in (compared with the RDPs). Besides, there is a low-frequency range where the emergence of RDPs and FDPs happens with an almost equal probability. Above these frequencies the reverse DPs may prevail, whereas below it is the forward DPs which dominate. The intersection peak (at 20–25 MHz on July 12, 2017) corresponds to the same number of FDPs and RDPs. Note that these conclusions are in good agreement with the results obtained from the DP observations of 2015 [2]. Using the spectral data obtained with the UTR-2, we have also analyzed the frequency drift rates of DPs on July 12 by fitting evolution of the peak of these bursts on the frequency-time plane. Just as in the case of [2], they follow a power-law function. In accordance with the histograms, the values K and ν have characteristically skewed distributions. Since the plasma mechanism of burst generation is considered to be the dominant one for the radiation of most radio bursts, the DPs probably draw their energy from the plasma waves that are created by the electron beams responsible for the storms of type III solar bursts. In particular, FDPs show a frequency dependence of their drift rate similar to that of Type III radio bursts and S bursts.

1.4. Heliographic results

Using the heliographic data of September 14, 2015, we have also investigated spatial properties of the DP (and the like) sources at 8–32 MHz by recording one frame every 3 s. For the studies of short bursts, this heliographic frame rate should be higher. But to make it higher, we would have to appeal to DSP waveforms, which is much more difficult for signal processing. To observe changes of source positions in the solar corona, there is no necessity in taking into account the entire abundance of frequency channels. Therefore, we used about 50 equidistant frequencies (occasionally, even less) in each frame. From the heliographic observations of DPs, we have found that the angular sizes of DPs were smaller than the beam size of the UTR-2. In particular, at 25 MHz they were below $25'$. Nevertheless, the heliograms allowed us identifying source positions of a variety of DPs (and likely) at fixed frequencies. This applies to both forward and reverse DPs. It is of interest that angular sizes of the type III burst sources observed during the storm together with the DPs also happened smaller than the UTR-2 beam size. Now, as long as the angular sizes of ordinary type III bursts are determined by radio wave scattering from inhomogeneous regions in the solar corona, the smaller angular sizes of DP sources (and their associated type III bursts) can testify in favor of a weaker coronal inhomogeneity above the emitting sources. By the way, this feature was accompanied by a weak solar activity. All this is consistent with the results of Suzuki and Gary (1979) obtained at a higher frequency. To provide for an angular resolution of DP component sources in this frequency range, special interferometer measurements would be preferred in the future.

2. Solar radio emission focused on ionospheric disturbances

2.1. Classification of spectral caustics from long-term radio data

Decameter radio observations are difficult not only because of the variety of radio interference of natural and artificial nature, but also because of the various manifestations of ionospheric effects. Most of the effects are well known. However, some of them remain unclear. It is no coincidence that, in order to avoid ambiguity, we use simultaneous observations

with several radio telescopes (UTR-2, URAN, GURT and others). Nevertheless, purposeful observations of the interaction of solar radio emission with the ionosphere are also of interest [7–9]. They permit of a better understanding of what can or cannot be expected from this interaction. An advanced study of the solar dynamic spectra perturbed as a result of focusing of the low-frequency emission by the Earth's ionosphere has been presented recently [7]. Using the data set obtained with the Nançay Decametric Array (NDA), we have performed a statistical analysis of the spectral structures in the solar dynamic spectra within the range of 10–80 MHz. We have detected certain structures in the spectral data from the NDA for 129 observation days from 1999 to 2015. The structures occur in the spectrograms as intensity variations different from the well-known solar radio bursts. The data set is useful because observations of the solar radio emission were performed every day, but spectral structures are detected less frequently. The URAN-2 was used for similar daily observations over a period of several years. For many of the events the sharp edges with enhanced intensity that appear on the spectrograms are distinctive characteristics of these structures. It is because of this spectral feature that they are called Spectral Caustics (SCs). Structures such as the Spectral Caustics are caused by natural focusing of solar radiation in the Earth's ionosphere. About 81% of all the days when SCs were detectable corresponded to active phases of solar cycles 23 and 24 (48 and 33%, respectively). Using the long-term observational data from the NDA, we have found a wide diversity of spectral forms of the SCs. Along with individual features, they also show general properties. Proceeding from the characteristic features present in the spectral morphology of all SCs, we have classified the SCs observed by the NDA as several types [7]. The prevailing type is what we denote as an inverted V. The distinctive attribute of this type of SC is the presence of sharp, double-branched envelopes of enhanced intensity. In contrast to the previous V type, such SCs take wedge-shaped form with a kind of broadening toward higher frequencies. The borders of these structures are not clearly cut. This type of SCs tends to appear during strong solar noise storms. The X like SCs combine some of the spectral properties of the two previous types. Say, the dynamic spectra of these structures with sharp borders initially show some narrowing toward

a point of convergence, and then a distinct broadening with frequency. The fiber like type of the SCs manifests itself in the form of bright filaments and/or lanes. Unlike the previous types, these features are characteristic by absence of any frequency broadening/narrowing, while maintaining their frequency width constant. The fringe like SCs are rather rare events. In dynamic spectrum a fringe-like structure takes the form of alternating stripes showing intensity enhancements and depressions. The fringe-like SC events are very complicated. They may appear together with other types of SCs. Our classification might be helpful for identifying unknown patterns in the solar dynamic spectra. We have found that the rate of occurrence of SCs in dynamic spectra depends on the phase of the solar cycle.

In addition to classifying the individual types of SCs, we identified several properties of SCs based on their manifestations in the solar dynamic spectra. The characteristic durations of the SCs can vary between 5 and 20 min, occasionally reaching values about 1 h. In the NDA radio records, the SCs appear at frequencies close to 10 MHz. It seems likely that the low-frequency boundary of the SCs is determined by the ionospheric cut-off. To assign an upper frequency limit to the SCs, we used a set of data obtained with the radio telescopes which cover higher frequencies than the NDA. According to the spectral data of the IZMIRAN for the range of 25–270 MHz, SCs can be recorded up to $f = 200$ MHz. The SCs can occur during solar burst events (such as continuum noise storms; type IV bursts; groups of type III bursts, and others). A closer examination of the activity level for one such "quiet" group has revealed that the SCs were in fact accompanied by flares or/and CMEs, while no radio bursts in the frequency range of the NDA were observed.

Owing to continuous observations of the Sun by the NDA, it has been possible to perform a statistical examination of the SC occurrence in the spectral data. It should be noted that calculating the total number of SCs presents a certain difficulty. In some cases, the spectral structures arising during strong solar noise storms may be considered as SCs or parts of the continuum emission. Besides, the SCs can appear in groups. Therefore, it is not always obvious whether a group represents a single complex event or consists of multiple SCs. Nevertheless, quite often we were able to detect more than one SC. The histogram pre-

senting the number of days with SC records, sampled along a time scale (years), shows two grouped blocks with maxima near 1999 and 2013, and a 3 year period (2008–2010) demonstrating none of observed SCs. This histogram shows solar cycle variations. Moreover, the histogram for months and years indicates that the SCs in the NDA dynamic solar spectra appear mainly in winter time (the months of December through February) and autumn (the months of October and November), with just one spring month (March). From April to September the SCs were detected in three cases only. The stable detection of SCs over certain periods supports the hypothesis about seasonal character of their occurrence.

2.2. Numerical simulations and comparison with experimental data

The traveling ionospheric disturbances (TIDs) represent one particular type of ionospheric irregularities. They arise in the course of propagation of acoustic gravity waves (AGWs) and represent wave-like electron density structures traveling through the ionosphere. The AGWs are believed to be generated by various natural or anthropogenic processes (like earthquakes, hurricanes, the moving solar terminator, auroral activity, powerful explosions, missile launches, ionosphere modification events, etc.) The TIDs are classified according to their spatial and temporal scales (wavelengths and periods), and horizontal velocities. Thus, TIDs spatial (> 1000 km) and temporal (~ 0.5 – 3.0 h) periods belong to the large-scale class, while those with spatial and temporal scales of 100 – 600 km and 0.25 – 1.0 h, respectively, are classified as the medium-scale class. TIDs can propagate as free wave modes, being reflected by the Earth's surface, or as as guided wave modes. The results of modeling the wave focusing by ionospheric inhomogeneities effect have been obtained for the first time in the art [8]. We have considered medium-scale traveling ionospheric disturbances (MSTIDs), applying a ray tracing technique. To simulate daytime MSTIDs in the Earth's ionosphere, we have considered typical gravity wave parameters, like a horizontal wavelength of 300 km, temporal period of 40 min (i.e., a 125 m s^{-1} phase velocity), and a South-East propagation direction with an azimuth of 135° from the North. The result of our model calculation shows that the MSTID pattern represents a periodic se-

quence of enhancements and depressions of electron concentration. Besides, the TID front in the vertical plane is inclined with respect to the propagation direction. This configuration is significant with respect to the TID focusing effect. The main results of the study represent dynamic spectra for different values of the solar elevation angle. Each dynamic spectrum includes a distinctive spectral perturbation in intensity that can be recognized as a SC. This is consistent with the result established here, namely that the focusing effect of TIDs during solar radio observations can produce similar spectral structures [7].

We have shifted in this study from an analysis of observational data to modeling. We used a ray tracing technique to compute radio beam trajectories in a MSTID-containing terrestrial ionosphere. Dynamic spectra have been obtained for the model structures consistent with the observed SCs. Thanks to such simulations, we are now able to identify four types of SCs among the five ones declared by our earlier study, including the inverted V-like, V-like, X-like, and fiber-like types. Before all, this suggests a reliable basis for SC classification; second, offers a correct numerical treatment of the problem; and third, stresses the need for additional studies to explain the last remaining SC type, that is, the fringe-like type. Based on the simulations, we found the dependence of the focusing frequency on the elevation angle of the Sun. The focusing frequency belongs to a characteristic point in the SC structure, which demonstrates a peak of intensity. The focusing frequency could be recorded if a ground-based observer were located near the focal point of the plasma lens created by a TID. Hence, by using the established relation, it should be possible to evaluate the frequency range within which a SC might appear. We have found that some of the SC records may be present in the spectrograms obtained for certain elevation angles of the Sun. The SCs can be generated at relatively low solar elevation angles ($< 25^\circ$). This range of elevation angles corresponds to seasons like late fall, winter, and early spring. This provides a nice explanation for the seasonal dependence in SC occurrence, which has been noticed previously [7]. According to these writers, 95% of the days when SCs are observable, belong to autumn or winter months. Moreover, we have found a close correlation between the slope of the TID front and the angle of incidence of the solar radiation passing through the ionosphere. This correlation con-

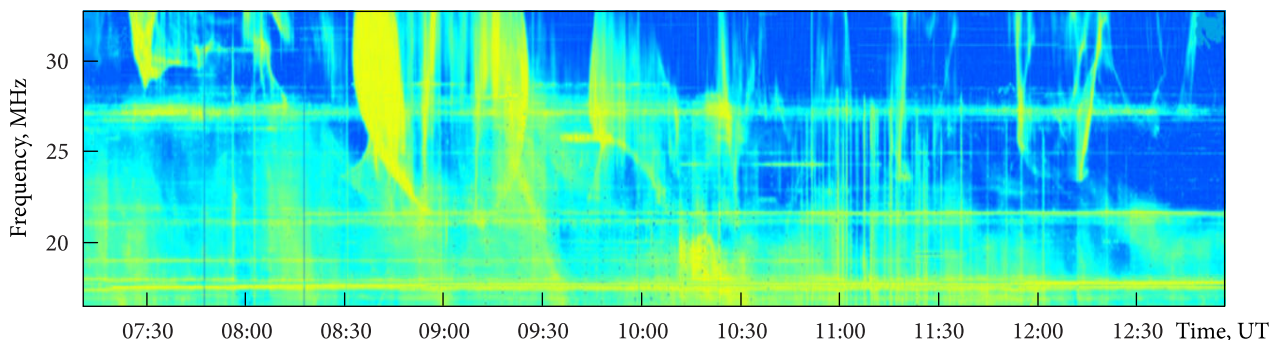


Fig. 2. Spectral caustics on the dynamic spectrum over 16.5 to 33 MHz as obtained with the URAN-2 on January 8, 2014

cerns spectral and morphological properties of SCs. In particular, the pattern of a SC is mostly symmetric in cases where the angle of incidence and the TID's inclination angle are close to each other. If there is a considerable difference between them, the pattern loses its symmetry, and envelopes and directions of rotation present in solar radio spectrograms are modified. From a careful review of earlier studies we concluded that the SC topic has not been fully investigated yet. The effect of solar radiation focusing is related to the specific phenomenon of propagation of solar radio waves through the terrestrial ionosphere. This natural effect is observed with ground-based radio instruments operating within the 10–200 MHz range, in the form of peculiar patterns (i.e., SCs) on the solar dynamic spectra. It was suggested that the SCs could be associated with MSTIDs. As a result, we were able to present the first direct observations of SCs induced by MSTIDs, using the solar dynamic spectra exhibiting SCs as obtained with different European radio telescopes on January 8, 2014. Also, simultaneous two-dimensional, detrended maps were obtained of the total electron content (dTEC) over Europe [9]. In that analysis we used the observations obtained with the URAN-2 array (Fig. 2), as well as with the NDA, several e-Callisto stations and IZMIRAN. All the instruments operated in overlapping frequency bands. The SCs can be recognized in the spectrograms by their distinctive spectral shapes. The most part of the SCs belong to the prevalent inverted V-like type. Some SCs appear in the form of lanes, corresponding to the fiber-like type. A few SCs cannot be clearly classified within the scheme presented in paper [6]. In order to explore the "parental" TID that causes an SC, we adopted the method that is generally used for TEC mapping. The ionosphere is represented as a thin layer (shell). Its alti-

tude is generally set equal to the height of the F2 peak (hmF2). The integrated magnitude of electron density within the F2 makes the main contribution to TEC values. Then, the TEC values obtained are ascribed to the so-called ionospheric pierce point (IPP), and mapped on the shell. The IPP represents the point at which the satellite-receiver line of sight crosses the ionosphere shell. Therefore, we can localize the place — the IPP position — where the line of sight between the Sun and the antenna crosses the ionospheric shell. That way, a set of IPP coordinates can be determined and plot on the dTEC maps over the lifetime of a particular SC. This allows us to observe directly the instantaneous dTEC structure and the position where the wavefront of the incident radio wave penetrates into the ionosphere. For the sake of simplicity, we will define the TID wavefront as a crest and the region between two successive wavefronts as a valley. The crests and valleys have high and low magnitudes of electron density, respectively. The focusing could only happen when the solar radio wave propagates through a valley where the refractive index is higher than such in the surrounding crests. Thus, we found that the IPP positions corresponding to any SC are contained within a valley on the dTEC map. If that is the case, we can identify the particular TID responsible for a specific SC. In all the cases considered, the timing analysis performed allowed us to reveal, with a lot of confidence, the facts of couplings between MSTIDs and SCs. We have proved that the peculiarities observed in spatial structure of TIDs on dTEC maps were consistent with time-frequency characteristics of the corresponding SCs in the spectrograms. In addition, our study has helped resolving the controversy about origin of SCs in the solar radio records, which might be mistakenly attributed to the Sun. In that work, we have demonstrated a collec-

tion of solar dynamic spectra obtained at meter- and decameter wavelengths by radio instruments around Europe. It is seen that SCs occur almost uniquely in each dynamic spectrum. Thus, the features of SCs are not of solar origin, rather being a consequence of interaction of solar radio emission with various inhomogeneities in the ionosphere.

3. Synchronized observations with space- and ground-based instruments

3.1. Advantages and disadvantages of space-based solar observations

Nowadays there is no doubt that astronomical and radio astronomical investigations performed from spacecraft and space missions are of extraordinary importance for science. It is sufficient to recall what a huge amount of new scientific data of interest does the famous space telescope Hubble provide on a daily basis and has already provided. Really, its location outside the Earth's atmosphere has made it possible to avoid harmful optical effects, opening a new window for exploration of the Universe. As a result, a natural desire arises to reach a success of a similar level through spacecraft observations in other frequency ranges. One of the rather difficult tasks for terrestrial observations is the study of cosmic radio emissions in the decameter and longer wavelength range. A huge amount of radio frequency interference of various kinds whose waves propagate around the world, plus the undesirable and only occasionally predictable ionospheric effects represent major obstacles to rapid development of the decameter-wavelength radio astronomy. Meanwhile, this branch of science could give answers to important many astrophysical problems of importance. However, launching a similar decameter-wavelength radio instrument (similar in the sense of efficiency) as the Hubble telescope, into the near-Earth space or to the far side of the Moon is, for the time being, an extremely complex and costly undertaking. The point is that the antenna sensitivity of such a radio telescope depends on its effective area (size), which is, in turn, dependent on the wavelength of the emission received. That is why these antennas are so huge at low-frequencies. The weight and dimensions of the vehicles launched so far are limited. Therefore, at the present time the space missions like WIND, STEREO, etc. that carry radio observations out, are equipped with just a few

whip antennas. Of course, the performance of these cannot be compared with the characteristics of space telescopes such as Hubble and the like. Although the spacecraft WIND is located at the Lagrangian point L1 between the Earth and the Sun, which is about 1.5 million km away from the Earth, its distance from the Sun is 99 times greater. Therefore, the WIND antenna receives only a 2% higher signal than it would have had on the Earth [10]. Meanwhile, increasing the size of a space-based antenna is problematic, whereas it looks quite real in the case of a ground-based antenna (for example, by way of having built an antenna array). The main advantages of space-based radio observations are their frequency range below the ionospheric cutoff and opportunities for observing the radio Sun in continuous operation. However, in this case the quality of the data turns out to be very low because of the low frequency-time resolution. Type II, III, and IV solar radio bursts are being currently observed at frequencies below 10 MHz in satellite-based experiments above the terrestrial plasmasphere. The success of these measurements is due to the fact that the bursts are often very intense and sufficiently long lasting. As follows from many ground-based observations, the diversity of solar radio bursts is much higher at low frequencies. Besides, they vary in such parameters as the radiated flux and frequency-time characteristics. Unfortunately, the capabilities of the equipment on board are limited with respect for such measurements, hence the fine structures of solar bursts, resulting from such observations, are indistinguishable. Nevertheless, synchronized observations with space- and ground-based instruments might, in some cases, be helpful in overcoming the problems.

3.2. Synergy of space- and ground-based studies

Without any doubt, realization of any simultaneous collaboration in the study of the Sun, the solar corona and the interplanetary medium by both remote and "in-situ" techniques and space- and ground-based monitoring is highly desirable [11, 12]. Of great interest are space observations coordinated with the work of ground-based radio telescopes for which the frequency range of 8–33 MHz borders or even overlaps with the frequency range of space instruments. Based on the objectives of the STEREO mis-

sion, its facilities and geometry, it should be pointed out some extra capabilities and advantages given by simultaneous space- and ground-based observations in closely lying and overlapping wavelength bands. This becomes especially noticeable, when a ground-based telescope has a better sensitivity and higher directivity in comparison with the space-based instruments. The measurements of solar bursts (using STEREO spacecraft with different locations in space), with comparison of their intensity permits one to: first, determine their radio emission directivity and source positions (under some model assumptions). However, for some parameters of maximum positions and beam widths used in the two-point measurement of intensities, there is an ambiguity in the determination of maximum positions. The problem could be resolved, for example, by organizing on the Earth a third point of intensity measurements, thus obtaining more reliable results [11]. When solar activity is at a minimum, the number of solar bursts and their intensity is distinctly reduced. The high sensitivity of the UTR-2 radio telescope, due to its large effective area and the parallel high-speed spectral analysis in the broad band, permits us easily to detect radio bursts with >0.01 sfu (more than ~ 100 Jy) in intensity [12]. Therefore, the records of the UTR-2 are useful as precursors for the detection of bursts and their analysis from the STEREO records. Such bursts appear almost at the detection limit of the STEREO-WAVES instrument. Other large radio telescopes (URAN, GURT) are also useful for such tasks.

The recent investigations of solar radio emission by the Ukrainian radio telescopes have established many new interesting features about the fine structure of solar radio bursts at decametre wavelengths (<30 MHz). It turns out to be quite diverse in the frequency-time domain for many types of solar bursts [4, 13–15]. This is impossible for radio telescopes with small antennas. Such events are very important for understanding radio emission mechanisms on the whole and for the solar-corona diagnostics in particular. The additional data are useful for the interpretation of results obtained with the space-based missions. The sensitivity of the STEREO instrument is insufficient to separate a contribution of radio emission from the quiet Sun (to the galactic background radiation). The emission clearly has a thermal character because of the coronal plasma heated up to the temperature close to $\sim 10^6$ K. Its intensity decreases

with decreasing frequency. Nevertheless, it is easily observable for the UTR-2 and URAN telescopes [16–18]. The antenna temperature of the solar corona radio-emission distinctly exceeds the level of fluctuations and corresponds approximately to the antenna temperature of the galactic background. From a radio astronomical point of view the solar corona is a very dynamic structure in its form, size and brightness for very low radio frequencies. In this connection it should be pointed out that the radio emission monitoring of the quiet Sun by ground-based facilities, accompanied by burst observations from spacecraft, is of interest in its own right. The detailed connection between the thermal emission in the global (and local) scale and the solar bursts has not yet been fully studied. The relatively high spatial resolution of the UTR-2 radio telescope (about 38 arcminutes at 20 MHz), the quick electronic scanning of the angular position of the antenna pattern and the heliographic regime allows us to determine the position and the motion of radio sources of any type in the solar corona. Radio emission of solar bursts observed by UTR-2 is usually generated by electron beams at heights in some solar radii. The joint observations of the Ukrainian radio telescopes together with space-based missions (Wind/Waves, STEREO, Parker Solar Probe) and their combined analysis, taking into account a lower radio-frequency range and determining the parameters of the solar radio-source directivity, makes it possible to trace the evolution of radio-emission sources and the development of wave processes over a wide range of distances from the Sun right up to the orbit of the Earth. It should be especially emphasized that the space- and ground-based investigations do not compete with each other. On the contrary, they can and must help each other to provide more effective solar observations for understanding astrophysical phenomena responsible for radio events detected.

The UTR-2, URAN-2, GURT radio telescopes were used in many experiments jointly with space-based missions. As a rule, they were successful always. Let us mention some of them. The detection of an absorption burst at 9–30 MHz has been reported [19]. In particular, instrumental noise, radiation from the galactic background, contributions from the radiation of the quiet Sun, a type II burst, and absorption against its background were successfully separated. This event was noticeable for WIND observations,

but without our ground-based observations it would be difficult to explain confidently the space data because of a less sensitivity of the WIND antenna. During the summer periods of 2007 and 2008 we observed solar bursts comparing our records of the data from the WIND and STEREO. Our observations show clearly that only the records of highest intensity could prove detectable if observed with the Wind/WAVES or STEREO instruments [10]. As for the results of observations with the UTR-2, they demonstrate quite apparently a more complicated (and therefore, and more detailed) structure of the event which developed in the solar corona. On the one hand, while the sensitivity of the WIND and STEREO instruments is not sufficient for detecting solar burst events at 2–16 MHz, the intensity of solar bursts increases quickly toward lower frequencies which makes the space-based observations effective. Therefore, it is not surprising that the burst group of August 18, 2007 was observable with the STEREO. The radiation pattern of the source of solar bursts' radio emission was established with the help of the STEREO and UTR-2 through analysis of the event of June 3, 2011 [11]. During the type III burst storm we could observe at 12:10 UT a burst with a high-frequency cut-off in the form of a "caterpillar". Its maximum flux observable with the UTR-2 at 24 MHz was attained about 10^3 sfu. That burst demonstrated a lot of bright fibers (up to 14) with a low frequency drift. The event was also recorded by the STEREO spacecraft, however with a lower frequency-time resolution. At the same time the spacecraft observed the Sun from lateral sides with respect to ground-based observatories. This allowed STEREO-A to receive solar radio emission from the central meridian (on 180°) towards the west, and STEREO-B recorded solar bursts from the central meridian towards the east on 180° . Taking into account their positions, we can assume that the event was generated on the west side of the Sun. Indeed, the active regions NOAA AR 11222 and AR 11224 were located on heliolongitudes 40° – 50° and 10° , respectively, behind the solar limb during observations from the Earth. The radio records of STEREO-A show that at 11:36 UT the active processes started with NOAA AR 11222 via an increase of its brightness and sizes, and continued for about two hours. In the region NOAA AR 11224 the activity started later (after 12:36 UT). Therefore, it is very likely that the unusual burst was caused by

NOAA AR 11222, and its source, according to the UTR-2 data, had a wide radio emission pattern. The results obtained confirm that in order to interpret space-based observations it is necessary to compare them with simultaneous (synchronous) solar observations of radio emission, using the largest ground-based low-frequency radio telescope. Without joint observations, the above results would hardly have been possible. All of these approaches allow reducing the number of errors and uncertainties in such experiments.

In addition, this approach increases reliability of the results obtained. Synchronized observations with the participation of space-based instruments and Ukrainian radio telescopes have been continued. In particular, adequate explanations of the solar radio bursts observed by the Parker Solar Probe (PSP) at the encounter phase play an important role in understanding the intrinsic properties of the emission mechanism in the solar corona. Using a subarray of the GURT together with the PSP radio records of solar observations on June 5, 2020, we have been able to directly detect the radio events initiated by the active region behind the solar limb observed by the PSP spacecraft [20]. The required solar radio bursts were found on the PSP spectrogram from position records of the PSP spacecraft near the Sun and analysis of the radio wave mutual delays shown by the space- and ground-based records. The absence of sunspots from the side of PSP creates favorable conditions for the propagation of radio waves from a dense solar loop toward quiet regions with low densities. The lower frequency-and-time resolution of the PSP receiver was compensated for simultaneous ground-based observations with the use of advanced antennas and receivers.

3.3. Prediction of solar activity at the wavelength of X-rays

Nowadays, the prediction of solar activity is very important for a number of reasons. The release of high-energy radiation, as well as particle acceleration may provoke damaging effects both for terrestrial and space-based technologies. Unlike the CMEs that can reach the Earth one to three days after their launch from the Sun (thus leaving enough time for their detection), the flare-related space weather effects occur at a much faster rate, actually within minu-

tes after the flare's onset. As a result, it can lead to serious threats to human security and/or work safety, including losses of operational power, aviation disruptions, losses of communication, and disturbance to (or loss of) satellite systems. Therefore, the development of solar flares prediction methods should be our highest priority, in particular about what concerns the amounts of their energy release and ways of minimizing their harmful effects. Solar radio astronomy also pursues interests of its own. An observation planned is not limited to operability tests of the equipment alone, but involves choice of data recording modes, time periods of observation, frequency-and-time resolution, and much more. Therefore, prior to starting an observation session, the radio astronomer would like to know what is to be expected during the upcoming observations. With regard to solar radio observations, this means which solar bursts can be expected and how they are related to solar processes. The Sun is a strong X-ray emitter. The solar atmosphere (solar corona) is much hotter than the solar surface, thus being a source of thermal (soft) X-rays. The solar X-rays can be completely absorbed in the D- and E-regions of the Earth's ionosphere, so satellite-borne equipment offers the only way for measuring that radiation. The space-borne observations of solar flare phenomena in X-rays have been going on since 1960s. After 1974 the broad-band X-ray emission of the Sun has been recorded almost continuously by the meteorological satellites operated by the NOAA, first the Synchronous Meteorological Satellite (SMS) and later on with the Geostationary Operational Environment Satellite (GOES). The solar X-ray flares data are widely available from the NOAA Space Environment Center's site. Therefore, studies of the long-term solar variability and solar activity predictions are issues of the day for solar physics, associated with a wide variety of space weather effects, like radio bursts, shock waves, magnetic perturbations, particle beams, and others. Solar activity is known to be correlated with flare activity, so a variety of flare properties (e.g., time of occurrence and intensity) could be taken into account when attempting predictions. The X-rays belonging to two wavebands (specifically, soft emissions at 1 to 8 Å and hard ones at 0.5 to 4 Å) are being measured by the GOES. We concentrated on the soft X-ray emission [21–23]. It is particularly sensitive to high-temperature plasma effects, and thus represents an important diagnostic tool

for studying coronal temperature distributions. Flux measurements of the soft X-rays performed before and during flare events provide a wonderful opportunity for studying soft X-ray characteristics in active coronal regions.

The magnetic field of the Sun is a key player in the spectacular events such as solar flares, sunspots, and coronal mass ejections, and in heating the solar corona to high temperatures. It is structured and manifests evolution over a wide range of both spatial and temporal scales. Every 11 years, the Sun passes through a period of fewer, smaller sunspots, prominences, and flares (solar minimum), moving toward a period of greater numbers of larger sunspots, prominences, and flares (solar maximum). The solar cycle of magnetic activity is expected to be a consequence of a dynamo process in which a dipole field produces a toroidal field from differential rotation (Ω -effect), while a twisting process produces a dipole field from the toroidal field (α -mechanism). Since the Sun's hot gases are controlled by magnetic fields, the X-ray emission may be an indicator of these changes, both globally and locally.

Recently, the autoregressive modeling such as fractional integrated moving average (ARFIMA) has been used to solve problems in the rapidly developing field of time-dependent astronomy. In particular, the ARFIMA process was considered as a candidate for extensive statistical studies of the soft X-ray solar emission [21]. The ARFIMA model represents a discretized-time analog of Langevin's fractional equation that takes into account the non-Gaussian statistics and long-range dependences (long-term memory), i.e. the events that are arbitrarily distant but still capable of strongly influencing one another. As for the physical arguments in favor of such an approach, one can say the following. The processes taking place in solar flares are associated with a complicated motion of charged particles (plasma) in magnetic and electric fields. That motion favors generation of fields and energy accumulation with further transformation into the energy of flares. The classical problem concerning the motion of a charged Brownian particle through magnetic and electric fields can be described in the framework of Langevin equations. However, in strongly non-equilibrium plasmas, where turbulence is a prevailing phenomenon, it is the non-Gaussian (Lévy) statistics of random forces that becomes dominant. As a consequence, the solar

data provide information on anomalous (non-Gaussian) diffusion and non-Maxwellian stationary states. Analysis of soft X-ray emission observations shows this time series to be of a rather complicated nature. It contains both long-term dependences and heavy-tailed effects. The former may be responsible for the appearance of a random number of strong flares at the background, while their repetition one after another. The most convenient model for their joint description is the ARFIMA time series. The model has allowed predicting the time series of solar soft X-ray flares for the period when solar activity was again near its maximum in 2010 through 2014. The ARFIMA-based model combines the autoregressive (AR) and the moving average (MA) models, introducing fractional integration (FI) which leads to the concept of a long-term (power law-like) memory in contrast to the autoregressive moving average (ARMA) model (of which the autocorrelation function demonstrates an exponentially fast decay).

Our data analysis was also focused then on the soft X-ray emission observed during the current solar minimum period (having lasted in 2017 from July to September [22]). We have found two different (active and inactive) states of the solar activity using the Hidden Markov Model (HMM). We show that in the periods of high-solar activity the energy distribution of solar soft X-ray flares can be well described by an ARFIMA-GARCH model, whereas in the case of low activity an ARFIMA model is best fitted. The generalized autoregressive conditional heteroskedasticity (GARCH) process (i.e. process with variable variance) takes into account the heteroskedastic effects which are typically observed in the form of clustered volatilities. The ARFIMA time series driven by GARCH noise are just called ARFIMA-GARCH processes. Switching from an inactive to an active state is caused by explosive phenomena in the Sun. The model describes the three effects detectable in our empirical studies. One of them is long-term dependent, whereas the second one describes variance changes with time, and the third effect corresponds to heavy-tailed distributions in the X-ray data. Moreover, the model takes into account the memory-associated effects in the soft X-ray emission owing to evolution of the solar magnetic field. All of this together has allowed us to suggest a statistically justified model for explaining the solar activity variability observable over the current minimum period. While developing

this approach, we have found that the HMM model can also be applied to data analysis including the X-ray records of GOES-13 and GOES-15 (from July, 2015 to June, 2017) [23]. To find the best configuration of our model for different cases of activity (low, moderate or high), we continue testing the model with solar data.

4. Observations below 8 MHz close to ionospheric cut-off

4.1. Development of ultra-long-wavelength antennas for radio astronomy

A promising direction of research in radio astronomy is connected with radio observations at extremely low frequencies that are still accessible from the Earth's surface. The promise of such studies was repeatedly noted by the pioneer of radio astronomy, Grote Reber. Such observations are difficult to carry out because of the strong contribution of ionospheric effects and harmful radio frequency interference. Notice that, although the observations with Ukrainian telescopes are performed in a frequency range that is close to the ionospheric cut-off, there still are frequencies which could be used for the observations, but they are not available for the telescopes. The best case is the GURT. Its lowest frequency in radio observations equals 8 MHz, whereas the UTR-2 and URAN can only observe from 9 or 10 MHz and higher. As for the frequency of the ionospheric cut-off in our area, it turns out to be lower, often 4 to 6 MHz in day time and going further down (even to 2 MHz) at night. Still, over the periods of high solar activity, the cut-off frequency can jump up to 10 MHz and higher. The interest of researchers toward extremely low frequencies is caused by the fact that the respective characteristics of radio emissions are but little known from the radio astronomical point of view, while space-based radio measurements offer poor results.

The problem can be viewed in different ways. The far side of the Moon is a unique zone for radio silence as it may offer opportunities for observing very low-frequency radiation of various space objects that are practically inaccessible for ground-based observations. The construction of a large scale radio array is not an easy task even on the Earth. As for other planets and moons, the task of building scientific instruments under their extreme conditions is a major challenge. A Ukrainian program of lunar explorations from space-

craft has been suggested by Shkuratov et al. [24, 25]. The mission would include a landing module with radio astronomy antennas on board. Shielded from the Earth by the Moon, the low-frequency antennas could provide for unique observations, wherein the orbital module would be equipped with certain remote-sensing instruments not previously used in space exploration of the Moon. A relay satellite with scientific payload, operating from an elongated orbit with a pericenter over the north pole (100 km above the surface) and apocenter over the south pole (altitude about 3000 km) would transmit the scientific data to the Earth. The lunar antenna array could carry out important studies of astrophysical objects at super long wavelengths. For instance, observations of solar flares of various types, coronal mass ejections, etc. performed in the radio spectrometer mode (from hundreds of kHz to 40 MHz), would be of particular interest. Overlapping frequencies in the range of 10–40 MHz will allow one to work together with ground-based radio telescopes (UTR-2, URAN, and GURT). Joint observations of astrophysical objects with the help of both lunar and terrestrial antennas, coordinated through a relay satellite, could be possible on a very long base (Earth-Moon distance). Prospective steps to solar studies with the help of radio observations on the far side of the Moon were considered by Stanislavsky et al. [4]. While developing that research program, we have produced an antenna prototype for the future ultra-long-wavelength lunar telescope. It can record radio emissions from cosmic objects both independently and as a part of an antenna array or interferometer. Its important advantage is the possibility of undergoing pre-tests on the Earth by way of receiving low frequency radio emissions close to the ionospheric cut-off and above. In this regard, the apparent interest in the development of small-sized active dipoles for low-frequency radio astronomy has noticeably intensified both theoretical and experimental studies of antenna technology, amplifiers and related components [5, 6]. During the fifteen years of operation of active dipoles within the GURT the ground-based radio array has revealed their reliability and validity for scientific applications. Such dipoles, while being small in size, provide optimal "radio astronomical sensitivity" which is obtained primarily due to the contribution of the amplifier temperature to the noise temperature of the active dipole. In this case the noise temperature of the active di-

pole is close to the antenna temperature as obtained from observations of the Galactic radio background. Thus, in-depth studies have been carried out on the development of an ultra-long-wave broadband antenna for radio astronomy, with the Moon seen as the future location of the device. We have studied the complex geometry of an active-dipole antenna, located above a partially conductive ground, by means of numerical simulations of the antenna prototype and measurements of its parameters [25]. As a part of these studies, the dipole and the amplifier were designed and manufactured as an active antenna, capable of receiving cosmic radiation in a frequency range like 4 to 70 MHz. Test measurements of the Galactic background radiation have been successfully performed on the Earth, specifically at the S.Ya. Braude Radio Astronomy Observatory, NASU. The spectral records of solar radio emissions were obtained with the DSP-Z receiver (the abbreviation stands for Digital Spectro-Polarimeters, type Z) which is a standard device for observations with the UTR-2. This has enabled a real-time Fast Fourier transform (FFT) analysis in two independent channels, with a frequency bandwidth of 0 to 33 MHz. Since the prototype antenna can receive radio emission up to 70 MHz, we applied a special technique for records of radio emission over a frequency band twice as wide as the receiver can perform in each channel separately. While one of the channels received radio signals in the frequency range of 4 to 33 MHz, the other operated within 33 to 66 MHz. Their combination gave the radio emission spectrum within 4 to 66 MHz, close to our observable frequency range. The frequency and time resolutions were standard for solar radio observations, namely 4 kHz and 100 ms, respectively.

4.2. Solar U-type burst and its association

First successful observations of solar radio emission, effectuated with the antenna prototype, were carried out on June 5, 2020 [27]. Although the summer of 2020 was characterized by a minimal solar activity, some manifestations of the activity did occur. On May 29, 2020, a solar flare which seemed the largest event of the kind over the period since October, 2017 marked the awakening of the Sun for a new cycle of activity. It was a M-class flare, and a new active area, namely the NOAA AR 12765, arose on the limb from the eastern side of the Sun on June 3, 2020. That active

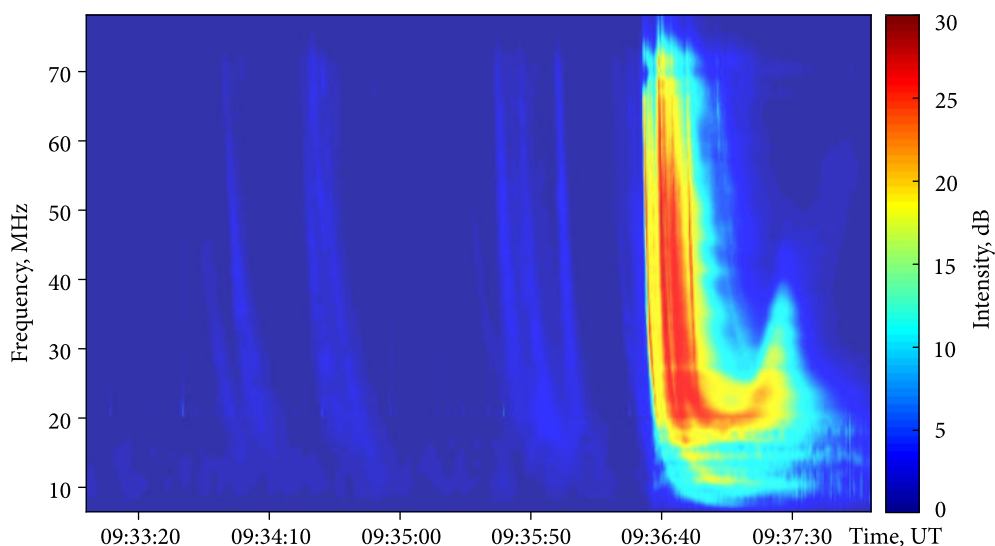


Fig. 3. Dynamic spectrum of the solar U+III association as observed with the GURT on June 5, 2020

region evolved from a single spot to a small bipolar region on June 5, 2020. The maximum size of the active region was 130 MH (millionth fractions of the visible solar hemisphere), which is comparable with the entire surface area of the Earth (almost 170 MH). During the following days the active region could be classified as the class β , although showing signs of decay. After June 10 it transformed to the class α , to enter later the far side of the Sun. Bipolar magnetic fields are of interest, before all, because they can be responsible for U-type solar radio bursts. Really, such a burst was observed on June 5, 2020 with the help of our antenna prototype, the GURT (Fig. 3) and many other radio telescopes (NDA and e-Callisto stations). An interesting feature of the event was its association with type III bursts, which were even interplanetary. Moreover, they were recorded with the space-based radio instruments WIND, STEREO and PSP. The change of sign, from negative to positive, in the frequency drift rate of the U burst was clearly seen in the frequency range from nearly 20 MHz to almost 15 MHz. Because of the generally low solar activity, the cut-off frequency of the Earth's ionosphere at our latitude is noticeably lower than 10 MHz (occasionally dropping down to 2 MHz). This makes it possible to carry out radio observations at frequencies that are quite close to those planned for recording sessions at lunar observatories. So, the bursts of our interest were reliably detected at extremely low frequencies (close to 6 MHz), despite numerous natural and artificial radio frequency interferences. A much

more detailed spectrum in the range above 8 MHz was obtained when the event was recorded by the GURT. As the sensitivity of the GURT array is higher than that of any dipole antenna, its dynamic spectrum represents many type III solar bursts (of lower intensities) that could be clearly visible prior to the U burst. Moreover, the latter had a fine structure. In that work we prepared several versions of the antenna prototype. In particular, one of them was characterized by an operating range of frequencies between 1 and 40 MHz. The use of such antennas allowed us to detect ionospheric cut off in a storm of type III solar bursts. Thus, we could combine two independent methods, namely vertical radio sounding of the ionosphere and radio astronomical observations of low-frequency type III solar bursts near their ionospheric cut-off. A time-frequency analysis of solar bursts and ionosonde measurements makes it possible to check the two methods for consistency [28]. Indeed, they are in agreement.

Conclusions

The UTR-2 cannot provide for polarization measurements, whereas the URAN-2 and GURT can. Such measurements are among the most difficult in the low-frequency radio astronomy, as they require careful calibrations and debugging. Our knowledge on polarization properties of solar bursts would make it possible to understand the mechanisms leading to generation of their various types that are observed.

On the other hand, solar bursts may be used as probing signals for investigating the solar corona. A perfect analysis of solar bursts would give information not only on their generation mechanism, but also on the medium (corona) which the radio emission propagates through. Currently, this is a task of unimaginable complexity because of insufficient knowledge of properties of the corona and generation mechanisms of the bursts.

The amount of natural and artificial radio interference in the low-frequency band of our observations does not decrease. That inflicts deteriorating effects on radio emission recordings. Our current efforts are aimed at improving the quality of the obtainable results through development of a variety of algorithms for selecting and correcting the corrupt data fragments in the frequency channels. It should be emphasized that the solar bursts of our interest and the interfering signals can be of comparable intensities. This makes their removal more difficult than in other cases. Nevertheless, the new methods promise success.

Sooner or later, radio telescopes will be on the far side of the Moon. The role of ground-based radio telescopes on the Moon, capable of performing observations at extremely low frequencies, close to the ionospheric cut-off, is hard to overestimate. On the one hand, they would start being informative immediately after being put in operation. An antenna ar-

ray ensures spatial selection against radio frequency interference. The correspondent radio records would be far better than such from a single active dipole, thus offering new results about solar radiation at these frequencies. On the other hand, in the future such an antenna could be involved in radio observations coordinated with Moon-based antenna observations. Therefore, the prior installation on the Earth of an array consisting of appropriate active dipoles would be doubly useful. It would be technically easier and less expensive than installing one on the Moon.

In our study of the decameter-band solar radio emission with the aid of Ukrainian radio telescopes we were oriented, before all, toward promotion of new research methods for understanding the processes responsible for thermal and sporadic components of solar radio emission, as well as their propagation in the solar corona at decameter and meter wavelengths. Our further observations of solar radio emissions, together with other ground-based radio telescopes and space instruments, would assist us in these studies in every way.

This work was supported by the Space Research program of the National Academy of Sciences of Ukraine (State registration numbers 0122U002459 and 0122U002460).

The authors are grateful to Prof. N.G. Shchukina for her useful comments.

REFERENCES

1. Volvach, Ya.S., Stanislavsky, A.A., Konovalenko, A.A., Koval, A.A., And Dorovsky, V.V., 2016. Comparative analysis of decametre "drift pair" bursts observed in 2002 and 2015. *Adv. Astron. Space Phys.*, **6**(1), pp. 24–27. DOI: 10.17721/2227-1481.6.24–27
2. Stanislavsky, A.A., Konovalenko, A.A., and Volvach, Ya.S., 2017. Frequency drift rate of solar decameter "drift pair" bursts. *Res. Astron. Astrophys.*, **17**(9), id. 097. DOI: 10.1088/1674-4527/17/9/97
3. Stanislavsky, A.A., Volvach, Ya.S., Konovalenko, A.A., and Koval, A.A., 2017. Solar drift-pair bursts. *Sun Geosph.*, **12**(2), pp. 99–103.
4. Stanislavsky, A.A., Konovalenko, A.A., Yerin, S.N., Bubnov, I.N., Zakharenko, V.V., Shkuratov, Yu.G., Tokarsky, P.L., Yatskiv, Ya.S., Brazhenko, A.I., Frantsuzenko, A.V., Dorovskyy, V.V., Rucker, H.O., and Zarka, P., 2018. Solar bursts as can be observed from the lunar farside with a single antenna at very low frequencies. *Astron. Nachr.*, **339**(7–8), pp. 559–570. DOI: 10.1002/asna.201813522
5. Stanislavsky, A.A., Bubnov, I.N., Konovalenko, A.A., Gridin, A.A., Shevchenko, V.V., Stanislavsky, L.A., Mukha, D.V., and Koval, A.A., 2014. First Radio astronomy examination of the low-frequency broadband active antenna subarray. *Adv. Astron.*, **2014**, id. 517058. DOI: 10.1155/2014/517058
6. Yerin, S., Stanislavsky, A., Bubnov, I., Konovalenko, A., Tokarsky, P., and Zakharenko, V., 2019. Small-sized radio telescopes for monitoring and studies of solar radio emission at meter and decameter wavelengths. *Sun Geosph.*, **14**(1), pp. 21–24. DOI: 10.31401/SunGeo.2019.01.03
7. Koval, A., Chen, Y., Stanislavsky, A., and Zhang, Q.-H., 2017. Traveling ionospheric disturbances as huge natural lenses: Solar radio emission focusing effect. *J. Geophys. Res. Space Phys.*, **122**(9), pp. 9092–9101. DOI: 10.1002/2017JA024080
8. Koval, A., Chen, Y., Stanislavsky, A., Kashcheyev, A., and Zhang, Q.-H., 2018. Simulation of focusing effect of traveling ionospheric disturbances on meter-decameter solar dynamic spectra. *J. Geophys. Res. Space Phys.*, **123**(11), pp. 8940–8950. DOI: 10.1029/2018JA025584

9. Koval, A., Chen, Y., Tsugawa, T., Otsuka, Y., Shinbori, A., Nishioka, M., Brazhenko, A., Stanislavsky, A., Konovalenko, A., Zhang, Q.-H., Monstein, Ch., and Gorgutsa, R., 2019. Direct observations of traveling ionospheric disturbances as focusers of solar radiation: Spectral caustics. *Astrophys. J.*, **877**(2), id. 98. DOI: 10.3847/1538-4357/ab1b52
10. Stanislavsky, A.A., Konovalenko, A.A., Rucker, H.O., Abranin, E.P., Kaiser, M.L., Dorovskyy, V.V., Mel'nik, V.N., and Lecacheux, A., 2009. Antenna performance analysis for decameter solar radio observations. *Astron. Nachr.*, **330**(7), pp. 691–697. DOI: 10.1002/asna.200911226
11. Konovalenko, A.A., Stanislavsky, A.A., Rucker, H.O., Lecacheux, A., Mann, G., Bougeret, J.-L., Kaiser, M.L., Briand, C., Zarka, P., Abranin, E.P., Dorovsky, V.V., Koval, A.A., Mel'nik, V.N., Mukha, D.V., and Panchenko, M., 2013. Synchronized observations by using the STEREO and the largest ground-based decametre radio telescope. *Exp. Astron.*, **36**(1–2), pp. 137–154. DOI: 10.1007/s10686-012-9326-x
12. Stanislavsky, A.A., Konovalenko, A.A., Zakharenko, V.V., Bubnov, I.N., Volvach, Ya.S., Dorovskyy, V.V., Koval, A.A., and Mylostna, K.Yu., 2016. Coordinated synchronous observations of Solar System objects using the ground- and space-based methods of low-frequency radio astronomy. *Space Sci. & Technol.*, **21**(4), pp. 51–55 (in Ukrainian). DOI: 10.15407/knit2015.04.051
13. Koval, A.A., Stanislavsky, A.A., Chen, Y., Feng, Sh., Konovalenko, A.A., and Volvach, Ya.S., 2016. A decameter stationary type IV burst in imaging observations on the 6th of September 2014. *Astrophys. J.*, **826**(2), id. 125. DOI: 10.3847/0004-637X/826/2/125
14. Stanislavsky, A.A., Konovalenko, A.A., Abranin, E.P., Dorovskyy, V.V., Lecacheux, A., Rucker, H.O., and Zarka, P., 2018. Revisiting the frequency drift rates of decameter type III solar bursts observed in July – August 2002. *Sol. Phys.*, **293**(11), id. 152. DOI: 10.1007/s11207-018-1374-6
15. Stanislavsky, A.A., Konovalenko, A.A., Koval, A.A., Dorovskyy, V.V., Zarka, P., and Rucker, H.O., 2015. Coronal magnetic field strength from decameter zebra-pattern observations: complementarity with band-splitting measurements of an associated type II burst. *Sol. Phys.*, **290**(1), pp. 205–218. DOI: 10.1007/s11207-014-0620-9
16. Stanislavsky, A.A., Koval, A.A., and Konovalenko, A.A., 2013. Low-frequency heliographic observations of the quiet Sun corona. *Astronom. Nachr.*, **334**(10), pp. 1086–1092. DOI: 10.1002/asna.201211839
17. Brazhenko, A.I., Koval, A.A., Konovalenko, A.A., Stanislavsky, A.A., Abranin, E.P., Dorovskyy, V.V., Melnik, V.M., Vashchishin, R.V., Frantsuzenko, A.V., and Borysyuk, O.V., 2012. Peculiarity of continuum emission from upper corona of the sun at decameter wavelengths. *Radio Phys. Radio Astron.*, **3**(3), pp. 187–196. DOI: 10.1615/RadioPhysicsRadioAstronomy.v3.i3.10
18. Konovalenko, O.O., Koshovyy, V.V., Lozynskyy, A.B., Stanislavsky, A.A., Shepelev, V.A., Ivantyshyn, O.L., Kharchenko, B.S., Lozynskyy, R.A., Brazhenko, A.I., Abranin, E.P., and Koval, A.A., 2012. Quiet Sun observations by URAN-2 and URAN-3 decameter radio telescopes during the solar eclipse of August 1, 2008. *Radio Phys. Radio Astron.*, **17**(4), pp. 295–300 (in Ukrainian).
19. Konovalenko, A.A., Stanislavsky, A.A., Abranin, E.P., Dorovsky, V.V., Mel'nik, V.N., Kaiser, M.L., Lecacheux, A., and Rucker, H.O., 2007. Absorption in Burst Emission. *Sol. Phys.*, **245**(2), pp. 345–354. DOI: 10.1007/s11207-007-9049-8
20. Stanislavsky, A.A., Bubnov, I.N., Koval, A.A., Yerin, S.N., 2022. Parker Solar Probe detects solar radio bursts related with a behind-the-limb active region. *Astron. Astrophys.*, **657**, A21. DOI: 10.1051/0004-6361/202141984
21. Stanislavsky, A.A., Burnecki, K., Magdziarz, M., Weron, A., and Weron, K., 2009. FARIMA Modeling of solar flare activity from empirical time series of soft X-ray solar emission. *Astrophys. J.*, **693**(2), pp. 1877–1882. DOI: 10.1088/0004-637X/693/2/1877
22. Stanislavsky, A.A., Burnecki, K., Janczura, J., Niczyj, K., and Weron, A., 2019. Solar X-ray variability in terms of a fractional heteroskedastic time series model. *Mon. Not. R. Astron. Soc.*, **485**(3), pp. 3970–3980. DOI: 10.1093/mnras/stz656
23. Stanislavsky, A., Nitka, W., Malek, M., Burnecki, K., and Janczura, J., 2020. Prediction performance of Hidden Markov modelling for solar flares. *J. Atmos. Sol.-Terr. Phys.*, **208**, id. 105407. DOI: 10.1016/j.jastp.2020.105407
24. Shkuratov, Y.G., Konovalenko, A.A., Zakharenko, V.V., Stanislavsky, A.A., Bannikova, E.Y., Kaydash, V.G., Stankevich, D.G., Korokhin, V.V., Vavriv, D.M., Galushko, V.G., Yerin, S.N., Bubnov, I.N., Tokarsky, P.L., Ulyanov, O.M., Stepkin, S.V., Lytvynenko, L.N., Yatskiv, Y.S., Videen, G., Zarka, P., and Rucker, H.O., 2018. Ukrainian mission to the Moon: how to and with what. *Space Sci. Technol.*, **24**(1), pp. 3–30 (in Ukrainian). DOI: 10.15407/knit2018.01.003
25. Shkuratov, Y.G., Konovalenko, A.A., Zakharenko, V.V., Stanislavsky, A.A., Bannikova, E.Y., Kaydash, V.G., Stankevich, D.G., Korokhin, V.V., Vavriv, D.M., Galushko, V.G., Yerin, S.N., Bubnov, I.N., Tokarsky, P.L., Ulyanov, O.M., Stepkin, S.V., Lytvynenko, L.N., Yatskiv, Y.S., Videen, G., Zarka, P., and Rucker, H.O., 2019. A twofold mission to the Moon: Objectives and payloads. *Acta Astronaut.*, **154**, pp. 214–226. DOI: 10.1016/j.actaastro.2018.03.038
26. Bubnov, I.N., Konovalenko, A.A., Tokarsky, P.L., Korolev, A.M., Yerin, S.N., and Stanislavsky, L.A., 2021. Creation and approbation of a low-frequency radio astronomy antenna for studying objects of the Universe from the far side of the Moon. *Radio Phys. Radio Astron.*, **26**(3), pp. 197–210 (in Ukrainian). DOI: 10.15407/rpra26.03.197
27. Stanislavsky, L.A., Bubnov, I.N., Konovalenko, A.A., Tokarsky, P.L., and Yerin, S.N., 2021. The first detection of the solar U+III association with an antenna prototype for the future lunar observatory. *Res. Astron. Astrophys.*, **21**(8), id. 187. DOI: 10.1088/1674-4527/21/8/187
28. Stanislavsky, A.A., Bubnov, I.N., Koval, A.A., Stanislavsky, L.A., Yerin, S.N., Zalizovski, A.V., Lisachenko, V.M., Konovalenko, O.O., Kalinichenko, M.M., 2023. Validation of F2-layer critical frequency variations in the ionosphere with radio observations of solar bursts. *J. Atmos. Sol.-Terr. Phys.*, **245**, id. 06056. DOI: 10.1016/j.jastp.2023.106056

Received 02.06.2022

О.О. Станиславський¹, А.О. Коваль², І.М. Бубнов¹, А.І. Браженко³

¹ Радіоастрономічний інститут НАН України
вул. Мистецтв, 4, м. Харків, 61002, Україна
E-mail: a.a.stanislavsky@rian.kharkov.ua

² Astronomical Institute of the Czech Academy of Sciences
Fričova 298, 251 65 Ondřejov, Czech Republic

³ Полтавська гравіметрична обсерваторія
Інституту геофізики ім. С.І. Субботіна НАН України
вул. Мясоедова, 27/29, м. Полтава, 36029, Україна

ДОСЯГНЕННЯ У ВИВЧЕННІ ДЕКАМЕТРОВОГО
РАДІОВИПРОМІНЮВАННЯ СОНЦЯ ЗА ДОПОМОГОЮ
УКРАЇНСЬКИХ РАДІОТЕЛЕСКОПІВ. Частина 2

Предмет і мета роботи. У другій частині роботи продовжено подання результатів досліджень сонячного радіовипромінювання, що виконувались за допомогою українських радіотелескопів протягом останніх 20 років. Зроблено наголос на необхідності розробки інструментів і методів для визначення природи радіовипромінювання Сонця на декаметрових хвилях.

Методи і методологія. У цих дослідженнях низькочастотні українські радіотелескопи УТР-2, ГУРТ і УРАН-2 застосовуються разом з іншими наземними та космічними інструментами для досягнення всебічного розуміння фізичних процесів у сонячній короні.

Результати. Розроблено методи та інструменти для досліджень сонячних радіосплесків на фоні сильних завад. Отримано унікальні дані стосовно джерел спорадичного радіовипромінювання Сонця, ролі ефектів поширення радіохвиль, а також впливу іоносфери на результати спостережень. Наведено найбільш вагомні спостережні та теоретичні результати досліджень низькочастотного радіовипромінювання Сонця за останні 20 років. Продемонстровано ефективність використання сонячного радіовипромінювання як зондувального сигналу для дослідження не тільки сонячної корони, а й іоносфери Землі, що дозволяє виявити вплив останньої на результати радіоастрономічних спостережень.

Висновки. Українські радіотелескопи метрового та декаметрового діапазонів є неперевершеними інструментами для досліджень Всесвіту в низькочастотному діапазоні радіохвиль. Завдяки своїм відмінним характеристикам вони роблять вагомий внесок у розвиток світової сонячної радіоастрономії.

Ключові слова: Сонце, декаметрове радіовипромінювання, радіочастотні сплески, корона, УТР-2, УРАН-2, ГУРТ.